2-2013

Computational Fluid Dynamic Simulations for Determination of Ventricular Workload in Aortic Arch Obstructions

Jessica S. Coogan
Stanford University

Frandics P. Chan
Stanford University

John F. LaDisa
Marquette University, john.ladisa@marquette.edu

Charles A. Taylor
Stanford University

Frank L. Hanley
Stanford University

See next page for additional authors

Journal of Thoracic and Cardiovascular Surgery, Vol. 145, No. 2 (February 2013): 489-495.e1. DOI.

Computational fluid dynamic simulations for determination of ventricular workload in aortic arch obstructions

Jessica S. Coogan
Department of Bioengineering, Department of Pediatrics, Stanford University, Stanford, CA
Frandics P. Chan
Department of Radiology, Department of Pediatrics, Stanford University, Stanford, CA
John F. LaDisa Jr.
Department of Biomedical Engineering, Marquette University, Milwaukee, WI
Charles A. Taylor
Department of Bioengineering, Department of Pediatrics, Stanford University, Stanford, CA
Frank L. Hanley
Department of Surgery, Department of Pediatrics, Stanford University, Stanford, CA

Jeffrey A. Feinstein
Department of Bioengineering, Department of Pediatrics, Stanford University, Stanford, CA
Division of Pediatric Cardiology, Department of Pediatrics, Stanford University, Stanford, CA

Abstract

Objective

The cardiac workload associated with various types of aortic obstruction was determined using computational fluid dynamic simulations.

Methods

Computed tomography image data were collected from 4 patients with 4 distinct types of aortic arch obstructions and 4 controls. The categorization of arch hypoplasia corresponded to the “A, B, C” nomenclature of arch interruption; a type “D” was added to represent diffuse arch hypoplasia. Measurements of the vessel diameter were compared against the normal measurements to determine the degree of narrowing. Three-dimensional models were created for each patient, and additional models were created for type A and B hypoplasia to represent 25%, 50%, and 75% diameter narrowing. The boundary conditions for the computational simulations were chosen to achieve realistic flow and pressures in the control cases. The simulations were then repeated after changing the boundary conditions to represent a range of cardiac and vascular adaptations. The resulting cardiac workload was compared with the control cases.

Results

Of the 4 patients investigated, 1 had aortic coarctation and 3 had aortic hypoplasia. The cardiac workload of the patients with 25% narrowing type A and B hypoplasia was not appreciably different from that of the control. When comparing the different arch obstructions, 75% type A, 50% type B, and 50% type D hypoplasia required a greater workload increase than 75% coarctation.

Conclusions

The present study has determined the hemodynamic significance of aortic arch obstruction using computational simulations to calculate the cardiac workload. These results suggest that all types of hypoplasia pose more of a workload challenge than coarctation with an equivalent degree of narrowing.

Abbreviation and Acronym

BSA body surface area

Aortic coarctation and other arch obstructions interfere with normal flow through the aortic arch. Previous studies have been performed to determine the hemodynamic significance of these obstructions.1, 2 However, “aortic coarctation” is often used to describe a spectrum of arch obstructions that could comprise both localized and diffuse narrowing that occur in different regions along the aorta. Some classifications have separated diffuse narrowing from localized narrowing, but no uniform classification exists. In one classification, Bonnet described adult coarctation as a localized narrowing distal to the ductus arteriosus, and infantile coarctation was characterized by diffuse narrowing proximal to the ductus.[3] In the present study, we refer to Bonnet's “infantile coarctation” as aortic hypoplasia, and “adult coarctation” as aortic coarctation. Although seemingly similar, aortic hypoplasia and aortic coarctation could have very different hemodynamic significance for the patient,

even if the degree of narrowing is similar. In the present study, we sought to define aortic hypoplasia according to the location and degree in reference to the normal anatomy.[4] Next, using computational simulations, we investigated the hemodynamic significance of the different types and degrees of aortic hypoplasia.

Computational fluid dynamic simulations have been used extensively in the past to determine the complex hemodynamics associated with various congenital heart defects, mainly focusing on the Fontan circulation.5, 6, 7, 8 Recently, simulation tools were developed to allow the first realistic computational studies of 3-dimensional hemodynamics in patients with aortic coarctation.9, 10, 11 One of these tools replicates the function of the left ventricle with a circuit model and allows for the interaction between a 3-dimensional vascular model and the heart.[9] From this circuit model, pressure-volume loops can be simulated, and the cardiac workload can be computed. This cardiac workload can then serve as a possible indicator of the hemodynamic severity of various aortic arch obstructions.

The current assessment of the severity of arch obstruction relies on measurements of the diameter narrowing or the pressure decrease across the obstruction.[12] However, a single determination of the percentage of narrowing might not be sufficient in cases of aortic hypoplasia, in which the narrowing is diffuse. In addition, late outcome morbidity is still present in many patients with repaired coarctation,13, 14 in whom a minimal pressure decrease would be expected. Thus, we propose the use of the cardiac workload as a metric for the hemodynamic severity of aortic arch obstruction. Because severe aortic coarctation is known to lead to heart failure if left untreated,14, 15 we used the severe aortic coarctation model as a benchmark for comparison when calculating the cardiac workload for the various types of aortic hypoplasia. In the present study, we sought to determine the cardiac workload associated with different types and degrees of aortic hypoplasia in the newborn population with the hope of aiding surgical decision making.

Methods

Patients

Computed tomography angiography image data were collected from 4 patients with various types of aortic arch obstruction and 4 body surface area (BSA)–matched controls. All data were collected with Stanford University institutional review board approval. We used a classification scheme based on the location of the narrowing just as in aortic arch interruption[16]: type A, distal to the left subclavian artery; type B, distal to the left common carotid artery; and type C, distal to the right innominate. We added a type D (distal to the aortic valve and representing diffuse hypoplasia). Type C is extremely rare and was not included in the present analysis. The 4 patients included 1 with type A, 1 with type B, 1 with type D, and 1 with coarctation. The 4 BSA-matched control patients were free of any cardiovascular disease. The computed tomography angiography image data were quantitatively analyzed to determine the aortic diameter at the sinotubular junction, proximal to the right innominate, distal to the left common carotid artery, distal to the left subclavian artery, and at the diaphragm. These measurements were then compared against the data collected by Aluquin and colleagues[4] at the same aortic locations for normal subjects to quantify the degree of narrowing. The computational models for the 4 patients and their respective BSA-matched controls are shown in Figure 1.

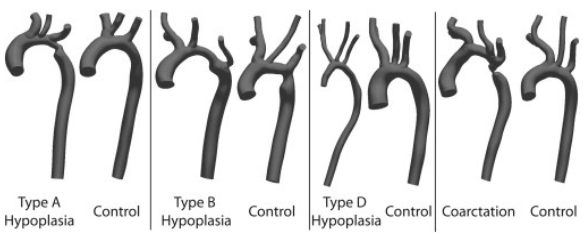

Figure 1. Three-dimensional models for each patient and corresponding body surface area *(BSA)*-matched control.

Imaging Processing

Three-dimensional patient-specific geometric models were constructed from the computed tomography angiography image data using custom software.[17] In brief, approximate centerline paths were defined through the vessels of interest, the vessel boundaries were identified along the vessel, and all the previously determined vessel boundaries were connected to create the model. A finite element mesh was created from this model by dividing the 3-dimensional model into linear tetrahedrons.[18] Additional models of type A and type B hypoplasia were created to represent tighter narrowing by scaling the entire hypoplastic segment until the desired degree of narrowing was achieved.

Numeric Simulation

The Navier-Stokes and continuity equations, representing conservation of momentum and mass of a Newtonian incompressible fluid, respectively, were solved on a finite element mesh of the 3-dimensional geometric model. The walls of the vessel were assumed to be deformable.[19] The simulation also requires the prescription of boundary conditions at the termination point of each vessel (outlet) in the 3-dimensional model.[20] These boundary conditions represent the vasculature that exists past each outlet and can be modeled with a simplified circuit model that represents the different components of the circulation. For the present analysis, a Windkessel model was prescribed at every outlet to represent the resistance of the proximal vessels, the capacitance of the proximal vessels, and the resistance of the distal vessels. In addition, a circuit model replicating the function of the heart was prescribed at the inlet of the model.[9] This heart model includes resistors and inductors that represent the aortic valves, a pressure source that represents the left atrial pressure, and a variable capacitance that represents the left ventricular elastance (contractility) of the heart (see Figure E1). The boundary conditions for each of the normal patients were chosen such that a realistic heart rate, blood pressure, cardiac output, and flow through the aortic branches were simulated. A realistic heart rate and blood pressure for each patient were determined according to the patient's age,21, 22 and a realistic cardiac output was determined by the BSA and an assumed cardiac index of 3.5 L/min/m^2.[22] Realistic flow was calculated by assuming the flow scales linearly with the vessel cross-sectional area[23]; this was confirmed in a separate set of 20 patients with coarctation.

Simulation Adaptation

When all boundary conditions remained the same between those with hypoplasia and the normal patients, the cardiac output and flow through the descending aorta are reduced, representing the result of a change in geometry alone. However, the body will adapt to the narrowing; thus, to mimic the physiologic cardiac adaptations, we maintained the boundary conditions at all outlets and only modified the heart model boundary condition to allow for 1 of 2 scenarios: (1) maintaining cardiac output, and (2) maintaining the flow through the descending aorta (hiatus flow) with respect to the control levels. These 2 adaptations were chosen because they might form a boundary within which the true physiologic state of the patient will lie. Maintaining cardiac output represents the “best case” scenario, because, at a minimum, the heart needs to supply the same amount of flow to the entire body, regardless of the presence of a stenosis. Maintaining hiatus flow represents the “worst case” scenario, because an increase in cardiac output greater than the normal level is required to maintain flow to the descending aorta such that renal perfusion remains constant. The heart model was modified by increasing the maximum left ventricular elastance (contractility) of the model and left atrial pressure in an iterative fashion until the desired cardiac output or hiatus flow was achieved. All other boundary conditions remained the same; thus, both adaptations could be satisfied by only a change in cardiac output. The cardiac workload of the heart was calculated by taking the area within the pressure-volume loop.

We also simulated another adaptation to represent a more physiologic state by incorporating vascular adaptation, such as vascular constriction of the cerebral vessels that is necessary to prevent overperfusion of the

brain tissue as cardiac output increases. This adaptation will help relieve some of the burden on the heart, because the excess flow to the cerebral vessels is diverted to the descending aorta to help increase renal perfusion. Thus, if a substantial increase in the flow to the aortic branch vessels was observed, the boundary conditions at the outlets of the branch vessels were modified to achieve a new target branch flow based on the vessel cross-sectional area while maintaining flow through the aortic outlet.

The preliminary results suggested that some of the simulations might result in unrealistic aortic pressure, cardiac output, and cardiac workload values, particularly in the models representing very tight narrowing. Thus, additional simulations were conducted for the tightest narrowing of the type A model, assuming a cardiac index of 2.5 L/min/m^2, which would reflect the lower limit of the cardiac index found in humans and would represent a degree of cardiac dysfunction not uncommon with severe aortic obstruction. All other methods remained the same.

Results

The patient characteristics of the 4 patients are listed in Table 1. The original geometry of type A and B hypoplasia represented a 25% diameter narrowing, type D hypoplasia represented 50% narrowing, and coarctation represented 75% narrowing. Additional models of type A and B hypoplasia were created to represent 50% and 75% narrowing. Figure 2 shows the pressure at the aortic inlet, the pressure-volume loop of the left ventricle, and the pressure and flow at the aortic outlet for the patient with coarctation. Realistic aortic pressure waveforms were simulated, with a loss of pulsatility seen in the flow and pressure distal to the coarctation. As expected, the simulation demonstrated an elevated mean and pulse pressure in the ascending aorta, regardless of the adaptations incorporated. The greatest mean and pulse pressure occurred when maintaining hiatus flow without vascular adaptation. The same trends were also seen in the patients with hypoplasia.

Table 1. Patient characteristics and associated clinical findings

Patient	Age (m)	Gender	Height (cm)	Weight (kg)	BSA (m^2)	Associated clinical findings
Type A	0.4	Female	45	2.5	0.17	Small perimembranous VSD, moderate aortic stenosis, mild mitral stenosis
Type B	0.2	Female	57	3.7	0.23	Small to moderate perimembranous VSD, tiny anterior midmuscular VSD
Type D	36	Male	92	15.3	0.61	Williams syndrome, bilateral branch pulmonary artery stenosis
Coarctation	8	Male	72	10.0	0.42	Subaortic membrane, bicuspid aortic valve, moderate aortic stenosis

BSA, Body surface area; VSD, ventricular septal defect.

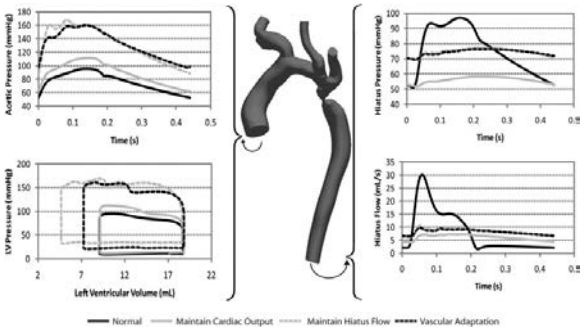

Figure 2. For the coarctation patient and body surface area–matched control, (*right*) aortic pressure measured at the inlet of the model and the pressure-volume loop of the left ventricle are shown. *Left*, Pressure and flow at the hiatus are shown. In each graph, results from the body surface area–matched control (normal) are shown with the results from the coarctation patient reflecting each of the different adaptations.

The cardiac workload was used as a metric to compare the significance of the different degrees and types of hypoplasia. The cardiac workload was normalized by determining the percentage of change in the workload from that of the BSA-matched control. The aortic pressure and percentage of change in workload for each patient under each adaptation is listed in Table 2. Compared with the control, coarctation required an increase in workload of 14.4% to maintain cardiac output and 132% to maintain hiatus flow. With vascular adaptation, the workload increased by 95% with respect to the control. The aortic pressure increased from the normal value of 95/53 to 112/61, 160/96, and 168/88 mm Hg to maintain cardiac output and hiatus flow with and without vascular adaptation, respectively.

Table 2. Aortic pressure and percentage of workload change associated with each adaptation and each type and degree of aortic obstruction

Obstruction type	**Narrowing (%)**	**Aortic pressure (mm Hg)**	**Workload change vs normal (%)**
Control			
Coarctation	0	95/53	0
Type A	0	82/50	0
Type B	0	82/50	0
Type D	0	91/55	0
Maintain cardiac output			
Coarctation	75	112/61	14.4
Type A	25	81/52	−1.2
	50	87/52	4
	75	102/60	17.3
Type A, lower cardiac output	75	99/57	18.1
Type B	25	85/50	2.2
	50	99/50	17.7
	75	142/72	64.4
Type D	50	122/52	34.7
Maintain flow			
Coarctation	75	168/88	132
Type A	25	82/53	−0.1
	50	93/56	16.8
	75	287/120	289
Type A, lower cardiac output	75	144/82	155
Type B	25	88/51	8.6
	50	107/54	34.9
	75	427/162	692
Type D	50	123/53	37.4
Maintain flow with vascular adaptation			
Coarctation	75	160/96	96

Type A	75	232/127	221
Type A, lower cardiac output	75	144/82	155
Type B	75	311/143	265

For type A hypoplasia, 25% and 50% narrowing did not result in appreciable changes in workload or pressure for any adaptation compared with coarctation. When maintaining cardiac output, the 75% narrowing geometry required a 17.3% increase in workload, comparable to the 14.4% increase seen with coarctation. To maintain hiatus flow without vascular adaptation, the workload increased by 289%; with vascular adaptation, the workload increased by 221%. The simulated aortic pressure for maintaining hiatus flow with and without adaptation was 232/127 and 287/120 mm Hg, respectively. These adaptations resulted in unrealistic values for workload and aortic pressure for an infant, motivating additional simulations with a reduced cardiac index.

When a cardiac index of 2.5 L/min/m^2 was assumed, the workload change and aortic pressure values were more reasonable. To maintain cardiac output, the workload increased by 18%. To maintain hiatus flow with and without vascular adaptation, the cardiac workload increased by 155% and the aortic pressure was 144/82 mm Hg for both cases.

The original type B hypoplasia represented a 25% narrowing and was also modified to represent 50% and 75% narrowing. The 25% narrowing geometry resulted in slight increases in aortic pressure and workload when maintaining both cardiac output and hiatus flow. The 50% narrowing case increased pressure and workload substantially when maintaining cardiac output, requiring a 17.7% increase in workload, comparable to that seen with coarctation. Maintaining the hiatus flow required an increase in workload of 34.9% with respect to the control. This increase was less than those seen for coarctation when maintaining hiatus flow, which can be explained because the left subclavian artery received a smaller percentage of the cardiac output than in the normal case, so that the descending aorta can receive more flow. The 75% narrowing case resulted in extremely large increases in workload for maintaining hiatus flow with and without adaptation (>200%) and an extremely high aortic pressure, both unrealistic for the infant population and indicating that left ventricular failure would likely be found in these patients.

Type D hypoplasia was characterized by a nearly uniform 50% narrowing of the entire aortic arch. Maintaining cardiac output resulted in large increases in the mean aortic pressure and an increase in the cardiac workload of 35% with respect to the control. This increase was larger than that seen for coarctation under the same adaptation condition. A 37% increase in workload was required to maintain the flow at the hiatus. Because no discrete narrowing was present, the workload associated with maintaining flow was not expected to be appreciably different from that associated with maintaining cardiac output. In this case, the branch flows were not appreciably different from the control case, and vascular adaptation was not simulated.

As shown with type B and D hypoplasia, the location of the narrowing or the absence of narrowing reduced the workload change associated with maintaining hiatus flow compared with coarctation. Thus, the workload change associated with maintaining cardiac output might represent the best method to compare each of the different types of hypoplasia. The percentage of increase in workload associated with maintaining cardiac output for each of the different types and degrees of aortic arch obstruction is shown in Figure 3.

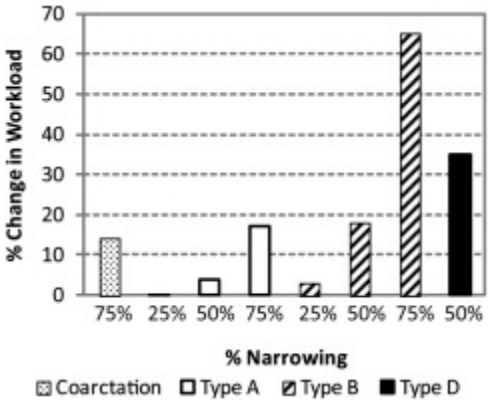

Figure 3. Comparison of the percentage of workload change required to maintain cardiac output for the different types and degrees of aortic obstruction.

Discussion

These results have demonstrated that we can successfully simulate realistic blood flow and pressure for a variety of different aortic arch obstructions. Using the simulation results, we can calculate the workload associated with aortic arch obstruction. The percentage of increase in workload was used as a metric for the hemodynamic significance of the narrowing.

The simulation results for coarctation revealed a workload increase of 14% to maintain cardiac output, 132% to maintain hiatus flow, and 96% to maintain hiatus flow with vascular adaptation. The range of workload increase with the different adaptations was large, but this could be expected, because we intended to model the theoretical bounds to the level of cardiac workload with maintaining cardiac output and hiatus flow. The workload associated with incorporating vascular adaptation lies within these bounds but closer to the adaptation to maintain hiatus flow, suggesting that the true physiologic workload of the patient will be closer to the upper bound of workload. One study also investigated the workload associated with aortic coarctation and found a left ventricular workload increase of around 50% between a normal group and an aortic coarctation group.[24] That study did not report the degree of stenosis of the aortic coarctation group; thus, a direct comparison with our study could not be made. However, a left ventricular workload increase of 50% also lies within the bounds defined by maintaining cardiac output and hiatus flow. In an additional study, left ventricular work was measured in normal patients and patients with aortic stenosis.[25] That study found that patients with an aortic valve gradient of 74 mm Hg, considered severe aortic stenosis, had a 98% greater left ventricular stroke work compared with normal patients.[25] Although the workload of aortic stenosis and aortic coarctation cannot be compared directly, we found that severe aortic coarctation requires an increased workload of up to 132%, similar to the increased workload seen with aortic stenosis.

Varying degrees of type A hypoplasia were simulated and the original geometry, representing a 25% diameter narrowing, required essentially no increase in workload for any of the adaptations. In a clinical setting, this patient might have been treated solely because a narrowing existed. Our findings suggest this narrowing poses no clinical significance in terms of cardiac workload. Even when the narrowing was increased to 50%, the increases in workload were still small compared with those with coarctation. However, when the narrowing was increased to 75%, the increases in workload were 17% and 289% for maintaining cardiac output and maintaining hiatus flow, respectively, and extremely high blood pressures were simulated. This might suggest that maintaining normal levels of flow through the descending aorta is not possible for this set of patients. With the additional simulations assuming a cardiac index of 2.5 L/min/m^2, the increase in workload was similar to that found for coarctation. Because a reduced cardiac output produces the same increases in workload as with the

coarctation case, we have concluded that 75% narrowed type A hypoplasia is more hemodynamically significant than 75% narrowed coarctation, which would be expected because the hypoplastic segment is longer than the discrete coarctation.

Varying degrees of type B hypoplasia were also simulated. Again, for the original geometry, representing 25% diameter narrowing, we found minimal change in the workload for any adaptation, even though the narrowing appeared quite significant. When maintaining cardiac output with 50% narrowing was simulated, the workload increased quite significantly and was similar to that required for coarctation and 75% type A hypoplasia. However, when modeling the adaptation to maintain hiatus flow, the workload required was not nearly as great as that required for coarctation or 75% type A hypoplasia. The location of the hypoplastic segment relieves some of the burden from the heart, because flow can be diverted directly from the left subclavian artery to the descending artery without passing any narrowing. With this added complexity, using the adaptation to maintain cardiac output might be the best method to compare the type B hypoplasia with coarctation and the other types of aortic hypoplasia. When comparing the workload associated with maintaining cardiac output, we found that 50% type B hypoplasia was more hemodynamically significant than coarctation and 75% type A hypoplasia.

Type D hypoplasia represents complete narrowing of the aortic arch. In this case, the workload associated with maintaining cardiac output was quite high compared with that for coarctation and the other types of hypoplasia. However, the workload to maintain hiatus flow was quite similar, because there was no discrete coarctation to pass to reach the aortic outlet that would change the distribution of cardiac output. Thus, using the adaptation to maintain cardiac output as the comparison point, we can conclude that 50% type D hypoplasia is more hemodynamically significant than coarctation, 75% type A hypoplasia, and 50% type B hypoplasia. In the present study, we chose not to model additional degrees of type D hypoplasia that might help determine when a patient should undergo surgery because no surgical solution exists for these patients.

Study Limitations

One limitation of the present study was that none of the adaptations modeled reflect the true physiologic adaptations that occur in response to aortic arch obstruction. However, the purpose of the study was not to determine the actual hemodynamics of each patient, but rather to compare the hemodynamics of the different types of obstruction. For this goal, we believe that simplifying the adaptations allowed more direct comparisons. The study was also limited by the small sample size. Although more patients would be ideal, the simulation process is complex and the patient population very small. However, we hope that the present study has demonstrated the power of computational simulations, because multiple different geometries were constructed from each patient that might may serve as a substitute for additional patients. Finally, many assumptions were made to determine the boundary conditions for the different models. At present, no methods are available to determine exactly what each boundary condition parameter should be for a particular patient. In particular, in this group of patients, only computed tomography scans were available, ruling out the possibility of using magnetic resonance imaging to acquire additional physiologic information. However, by using the same outlet boundary conditions between each patient and their respective controls and focusing on the changes in each hemodynamic parameter from the control value, we have removed some of the variability associated with the specific boundary conditions chosen. Once more physiologic information about specific patients becomes available, future studies can easily incorporate this information into the current method to yield more patient-specific simulations.

Conclusions

In the present study, we used computer simulations to model the blood flow in patients with various aortic arch obstructions. By calculating the workload associated with each obstruction, we compared the hemodynamic significance of aortic coarctation and various types of aortic hypoplasia. We found that the

workload associated with all types of aortic hypoplasia was larger than that for aortic coarctation of equivalent narrowing. The present study represents the first exploratory work to use computational simulations to understand a variety of different aortic arch obstructions and demonstrates a framework from which to build more realistic and patient-specific simulations.

Appendix

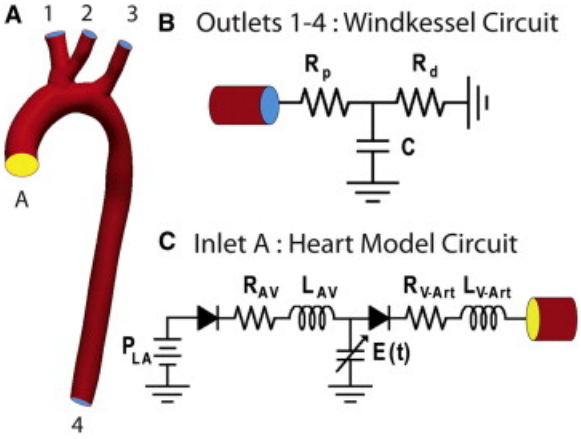

Figure E1. A, Three-dimensional model with inlet shown in *yellow* and labeled "A" and outlets shown in *blue* and labeled "1" to "4". B, Outlets 1 to 4 are coupled to the Windkessel model. C, Inlet A is coupled to the heart model. R_p, Resistance of proximal, larger vessels; R_d, resistance of distal, smaller vessel; *C,* capacitance of proximal, larger vessels; P_{LA}, left atrial pressure; R_{AV}, mitral valve resistance; L_{AV}, mitral valve inductance; *E(t),* left ventricular elastance; $R_{V\text{-}Art}$, aortic valve resistance; $L_{V\text{-}Art}$, aortic valve inductance.

References

1 M.F. O'Rourke, T.B. Cartmill. **Influence of aortic coarctation on pulsatile hemodynamics in the proximal aorta.** *Circulation*, 44 (1971), pp. 281-292

2 A.W. Aldousany, T.G. DiSessa, B.S. Alpert, S.E. Birnbaum, E.S. Willey. **Significance of the Doppler-derived gradient across a residual aortic coarctation.** *Pediatr Cardiol*, 11 (1990), pp. 8-14

3 W.T. Mustard, R.D. Rowe, J.D. Keith, A. Sirek. **oarctation of the aorta with special reference to the first year of life.** *Ann Surg*, 141 (1955), pp. 429-436

4 V.P.R. Aluquin, D. Shutte, M.R. Nihill, A.Y. Lu, L. Chen, J. Gelves, *et al.* **Normal aortic arch growth and comparison with isolated coarctation of the aorta.** *Am J Cardiol*, 91 (2003), pp. 502-505

5 A.L. Marsden, A.J. Bernstein, V.M. Reddy, S.C. Shadden, R.L. Spilker, F.P. Chan, *et al.* **Evaluation of a novel Y-shaped extracardiac Fontan baffle using computational fluid dynamics.** *J Thorac Cardiovasc Surg*, 137 (2009), pp. 394-403

6 M.R. De Leval, G. Dubini, F. Migliavacca, H. Jalali, G. Camporini, A. Redington, R. Pietrabissa. **Use of computational fluid dynamics in the design of surgical procedures: application to the study of competitive flows in cavopulmonary connections.** *J Thorac Cardiovasc Surg*, 111 (1996), pp. 502-513

7 E.L. Bove, M.R. de Leval, F. Migliavacca, R. Baalossino, G. Dubini. **Toward optimal hemodynamics: computer modeling of the Fontan circuit.** *Pediatr Cardiol*, 28 (2007), pp. 477-481

8 F. Migliavacca, R. Balossino, G. Pennati, G. Dibini, Y. Hsia, M.R. de Leval, *et al.* **Multiscale modelling in biofluidynamics: application to reconstructive paediatric cardiac surgery.** *J Biomech*, 39 (2006), pp. 1010-1020

9 H.J. Kim, I.E. Vignon-Clementel, C.A. Figueroa, J.F. LaDisa, K.E. Jansen, J.A. Feinstein, *et al.* **On coupling a lumped parameter heart model and a three-dimensional finite element aorta model.** *Ann Biomed Eng*, 37 (2009), pp. 2153-2169

10 J.F. Ladisa, C.A. Taylor, J.A. Feinstein. **Aortic coarctation: recent developments in experimental and computational methods to assess treatments for this simple condition.** *Prog Pediatr Cardiol*, 30 (2010), pp. 45-49

11 J.S. Coogan, F.P. Chan, C.A. Taylor, J.A. Feinstein. **Computational fluid dynamic simulations of aortic coarctation comparing the effects of surgical- and stent-based treatments on aortic compliance and ventricular workload.** *Catheter Cardiovasc Interv*, 77 (2011), pp. 680-691

12 J.C. Nielsen, A.J. Powell, K. Gauvreau, E.N. Marcus, A. Prakash, T. Geva. **Magnetic resonance imaging predictors of coarctation severity.** *Circulation*, 111 (2005), pp. 622-628

13 M. Cohen, V. Fuster, P.M. Steele, D. Driscoll, D.C. McGoon. **Coarctation of the aorta: long-term follow-up and prediction of outcome after surgical correction.** *Circulation*, 80 (1989), pp. 840-845

14 N.P. Jenkins, C. Ward. **Coarctation of the aorta: natural history and outcome after surgical treatment.** *Q J Med*, 92 (1999), pp. 365-371

15 M. Campbell. **Natural history of coarctation of the aorta.** *Br Heart J*, 32 (1970), pp. 633-640

16 R.L. Collins-Nakai, M. Dick, L. Parisi-Buckley, D.C. Fyler, A.R. Castaneda. **Interrupted aortic arch in infancy.** *J Pediatr*, 88 (1976), pp. 959-962

17 N. Wilson, K. Wang, R.W. Dutton, C.A. Taylor. **A software framework for creating patient specific geometric models from medical imaging data for simulation based medical planning of vascular surgery.** *Lect Notes Comput Sci*, 2208 (2001), pp. 449-456

18 O. Sahni, J. Muller, K.E. Jansen, M.S. Shephard, C.A. Taylor. **Efficient anisotropic adaptive discretization of the cardiovascular system.** *Comput Methods Appl Mech Engrg*, 195 (2006), pp. 5634-5655

19 C.A. Figueroa, I.E. Vignon-Clementel, K.C. Jansen, T.J.R. Hughes, C.A. Taylor. **A coupled momentum method for modeling blood flow in three-dimensional deformable arteries.** *Comput Methods Appl Mech Engrg*, 195 (2006), pp. 5685-5706

20 I.E. Vignon-Clementel, C.A. Figueroa, K.E. Jansen, C.A. Taylor. **Outflow boundary conditions for three-dimensional finite element modeling of blood flow and pressure in arteries.** *Comput Methods Appl Mech Engrg*, 195 (2006), pp. 3776-3796

21 J.W. Custer, R.E. Rau (Eds.), *The Harriet Lane Handbook: A Manual for Pediatric House Officers*, Elsevier Mosby, Philadelphia (2009)

22 **Task force 1987 on blood pressure control in children: report of the second task force on blood pressure control in children.** *Pediatrics*, 79 (1987), pp. 1-25

23 M. Zamir, P. Sinclair, T.H. Wonnacott. **Relation between diameter and flow in major branches of the arch of the aorta.** *J Biomech*, 25 (1992), pp. 1303-1310

24 T.P. Graham, B.W. Lewis, M.M. Jarmakani, R.V. Canent, M.P. Capp. **Left heart volume and mass quantification in children with left ventricular pressure overload.** *Circulation*, 41 (1970), pp. 203-212

25 J.W. Kennedy, J. Doces, D.K. Steward. **Left ventricular function before and following aortic valve replacement.** *Circulation*, 56 (1977), pp. 944-950

This study was supported by a National Science Foundation graduate student fellowship and Benchmark Fellowship in Congenital Cardiovascular Engineering in association with the Vera Moulton Wall Center at Stanford University.

Disclosures: Dr LaDisa, Jr, reports consulting and lecture fees for Medtronic Cardiovascular. The other authors have nothing to disclose with regard to commercial support.